

Supporting information for

Analysis and visualization of quantitative proteomics data using FragPipe-Analyst

Yi Hsiao¹, Haijian Zhang², Ginny Xiaohe Li³, Yamei Deng³, Fengchao Yu³, Hossein Valipour Kahrood^{2,4}, Joel R. Steele², Ralf B. Schittenhelm^{2,4}, and Alexey I. Nesvizhskii^{1,3,}*

¹Department of Computational Medicine and Bioinformatics, University of Michigan, Ann Arbor, MI 48109, USA,

²Monash Proteomics & Metabolomics Platform, Department of Biochemistry and Molecular Biology, Biomedicine Discovery Institute, Monash University, Clayton, Victoria 3800, Australia,

³Department of Pathology, University of Michigan, Ann Arbor, MI 48109, USA,

⁴Monash Bioinformatics Platform, Department of Biochemistry and Molecular Biology, Biomedicine Discovery Institute, Monash University, Clayton, Victoria 3800, Australia.

Supplementary figure S1. PCA plot by batch of ccRCC proteomics dataset collected by TMT.

Supplementary figure S2. Missing value heatmap of ccRCC proteomics dataset collected by TMT.

Supplementary figure S3. Over representation test result for downregulation part in tumors vs NAT comparison of ccRCC proteomics dataset collected by TMT.

Supplementary figure S4. PCA plot of ccRCC proteomics dataset collected by data-independent acquisition (DIA).

Supplementary figure S5. Correlation heatmap of ccRCC proteomics dataset collected by DIA.

Supplementary figure S6. Volcano plot (left) and overrepresentation test result (right) of ccRCC proteomics dataset collected by DIA.

Supplementary figure S7. Scatter plot shows comparison of log₂ fold changes obtained from DIA and TMT experiments when comparing tumors versus NATs.

Supplementary figure S8. Density plot shows the imputation effect on AP-MS experiments used here.

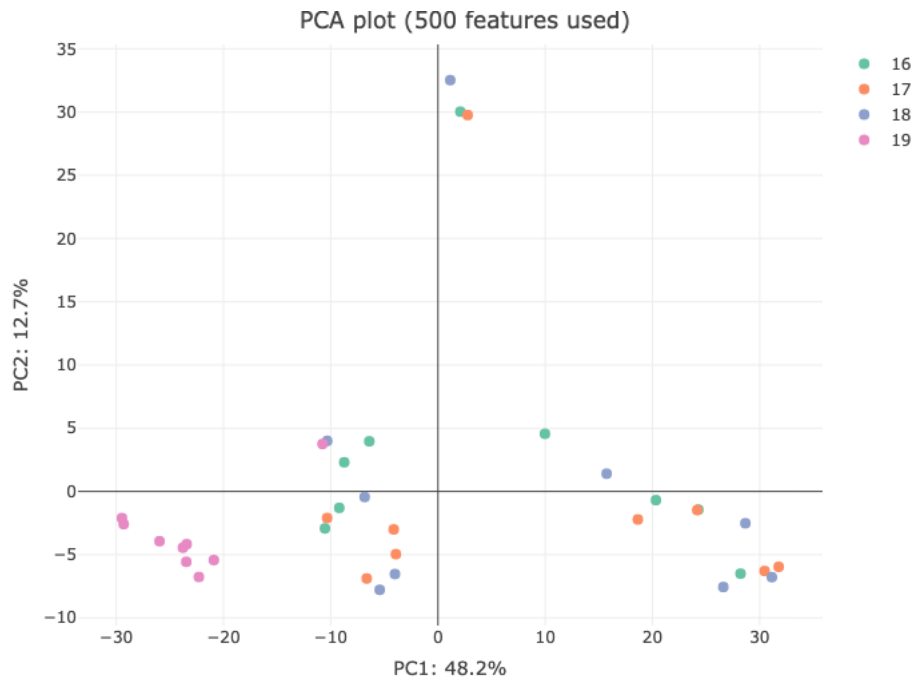
Supplementary figure S9. Network visualization of HNSCC AP-MS dataset generated by SAINTexpress.

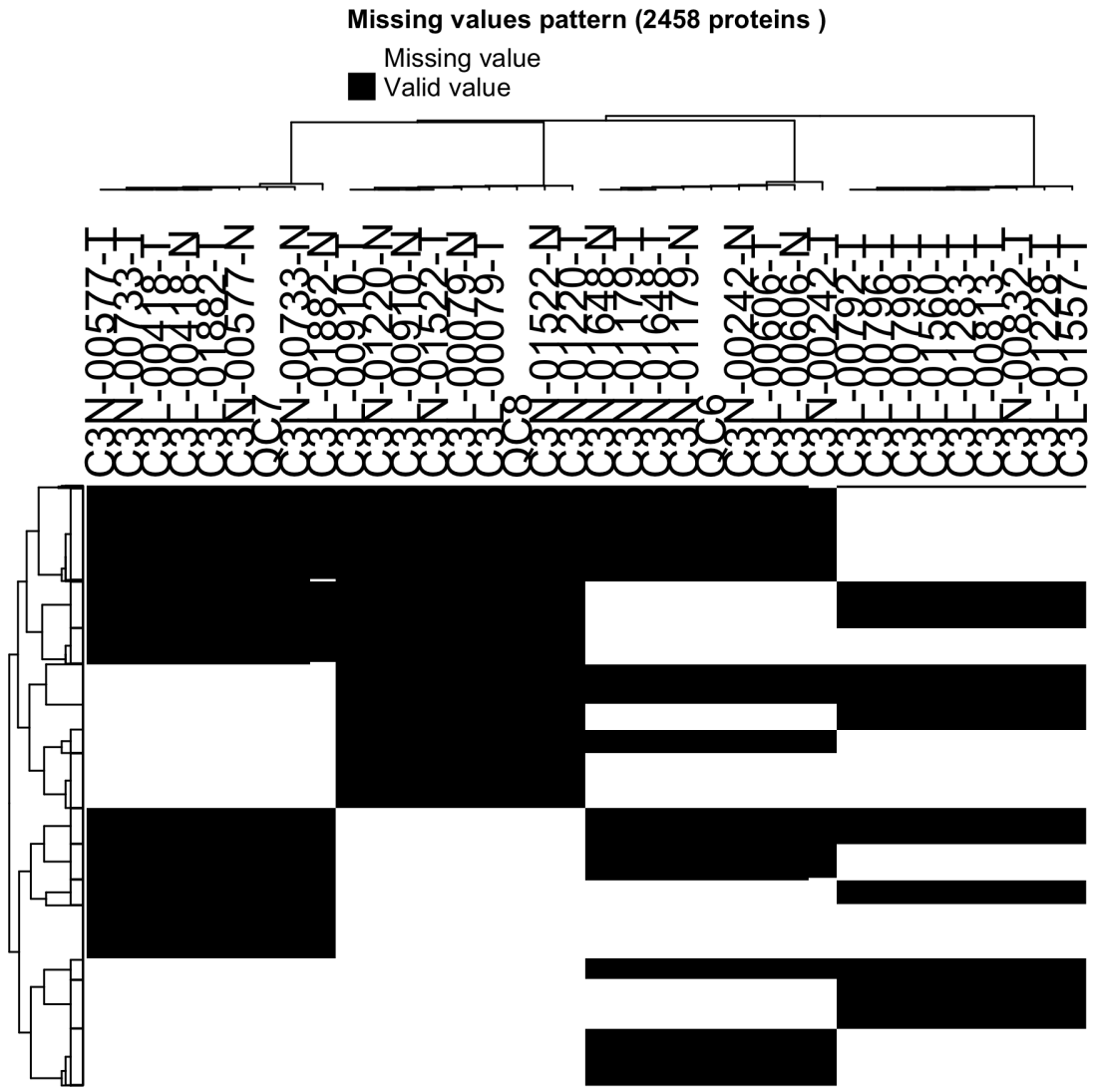
Supplementary figure S10. PCA plot of peptide-level analysis on ccRCC proteomics dataset.

Supplementary figure S11. Correlation matrix plot of ccRCC proteomics dataset using peptide-level quantification result.

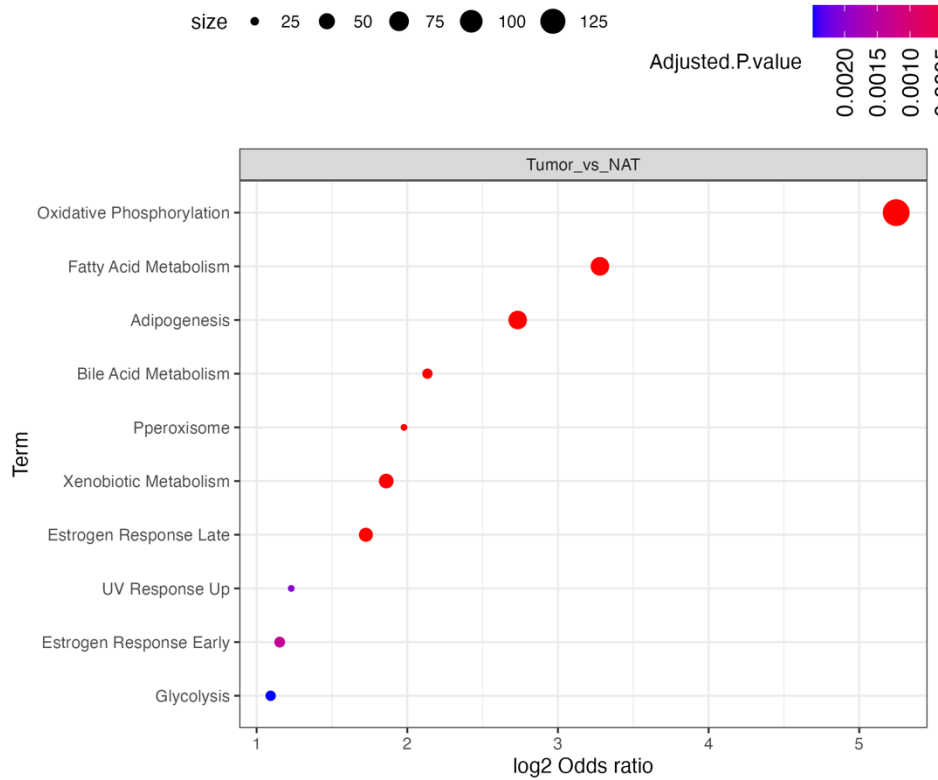
Supplementary figure S12. Volcano plot (left) and overrepresentation test result (right) of peptide-level analysis on ccRCC proteomics dataset.

Supplementary figure S13. PCA plot of ccRCC phosphoproteomics dataset after normalization.

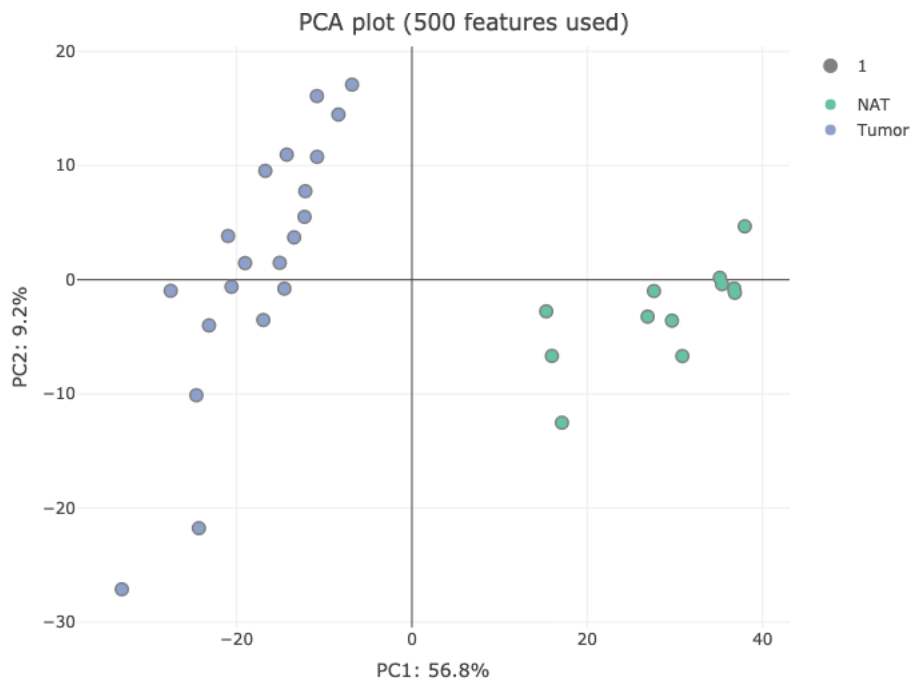




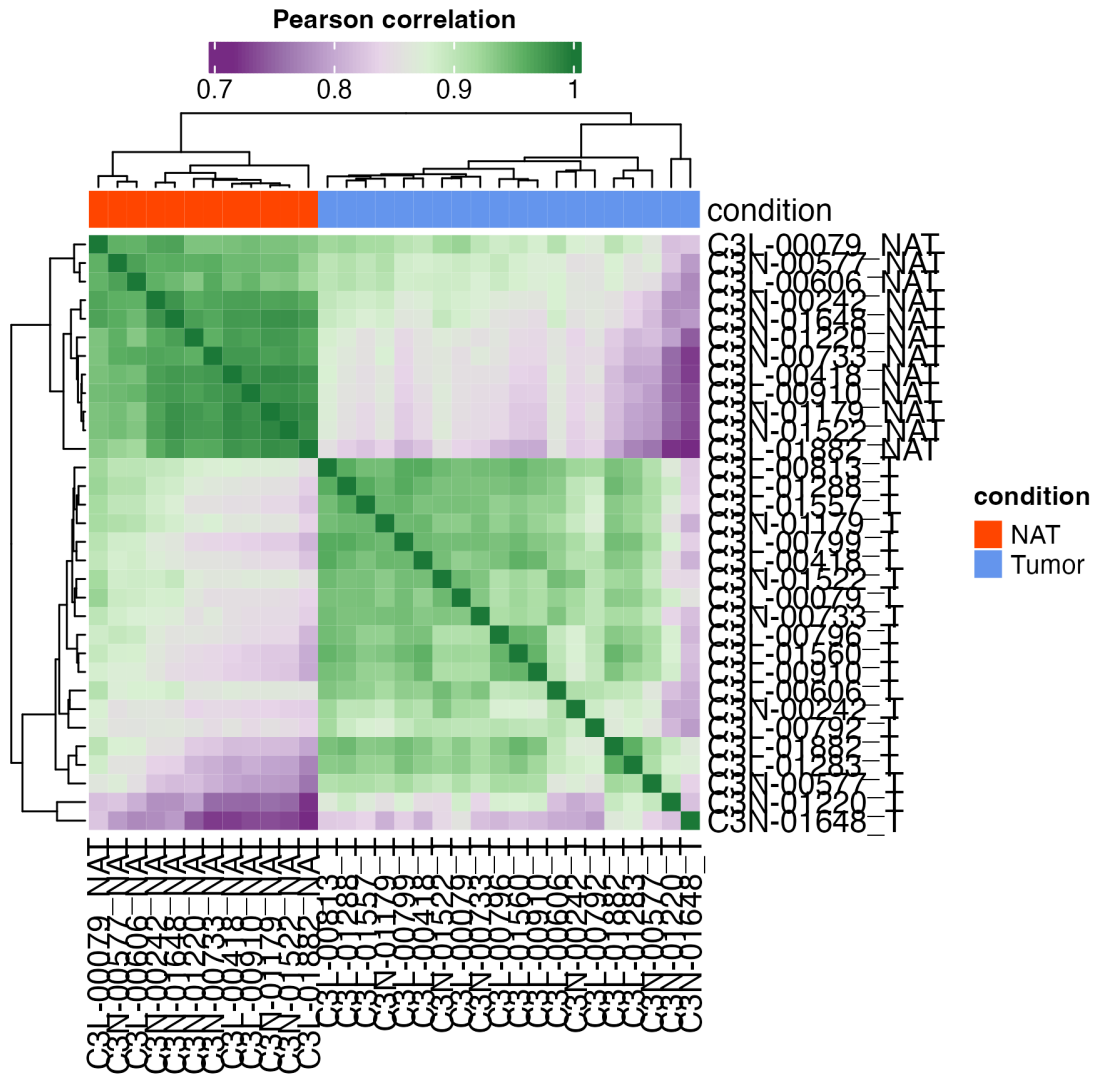
Supplementary figure S2. Missing value heatmap of ccRCC proteomics dataset collected by TMT.



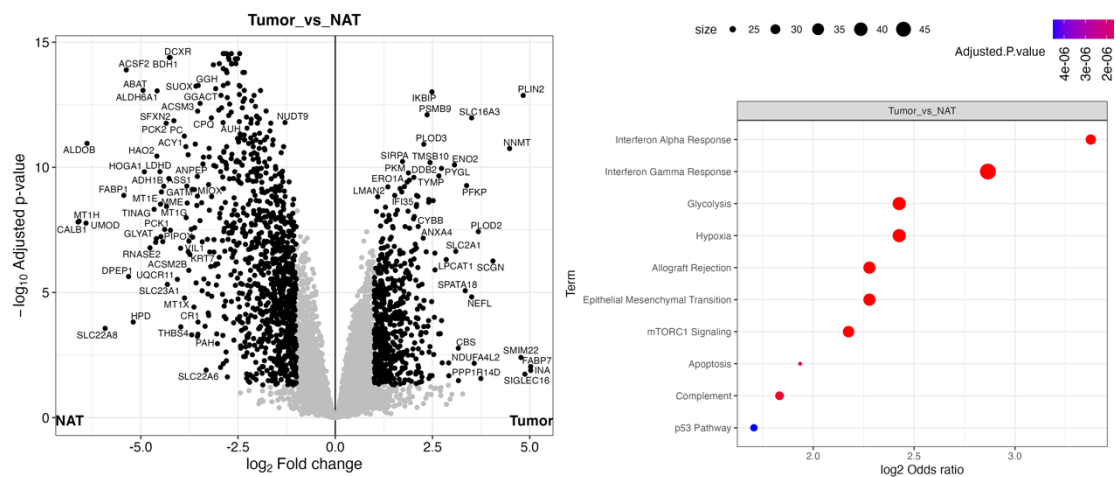
Supplementary figure S3. Over representation test result for downregulation part in tumors vs NAT comparison of ccRCC proteomics dataset collected by TMT.



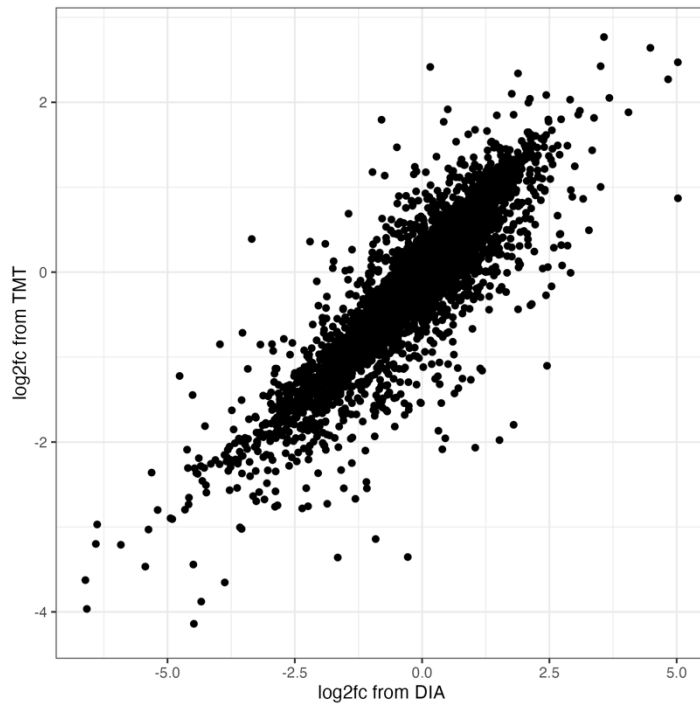
Supplementary figure S4. PCA plot of ccRCC proteomics dataset collected by data-independent acquisition (DIA).



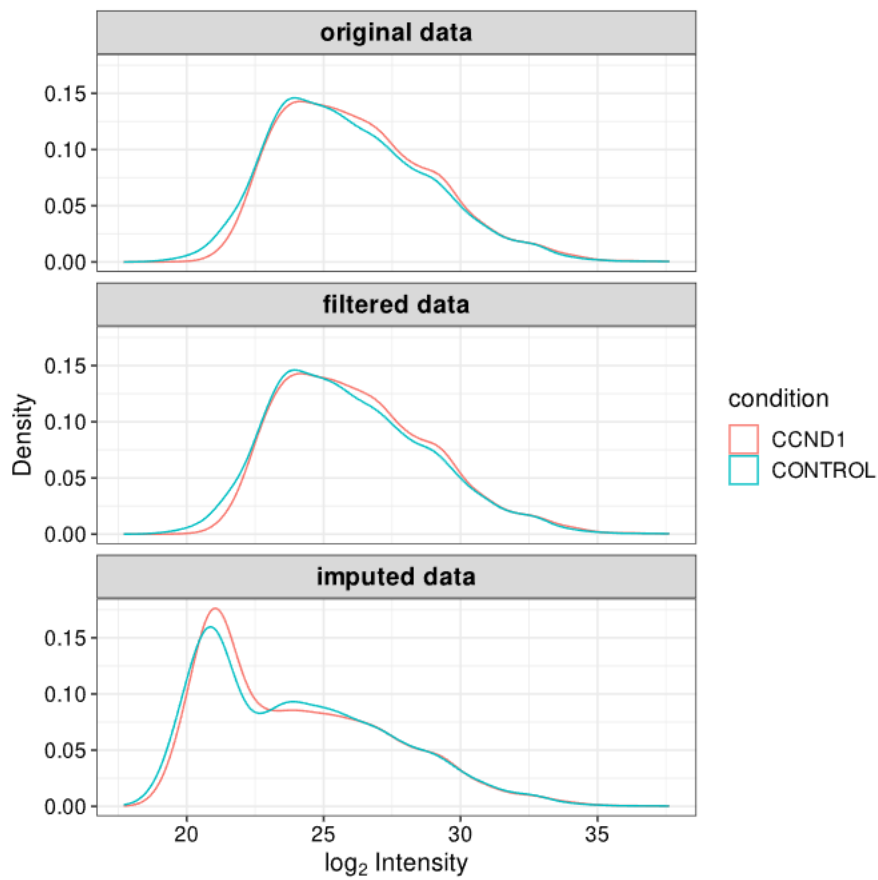
Supplementary figure S5. Correlation heatmap of ccRCC proteomics dataset collected by DIA.



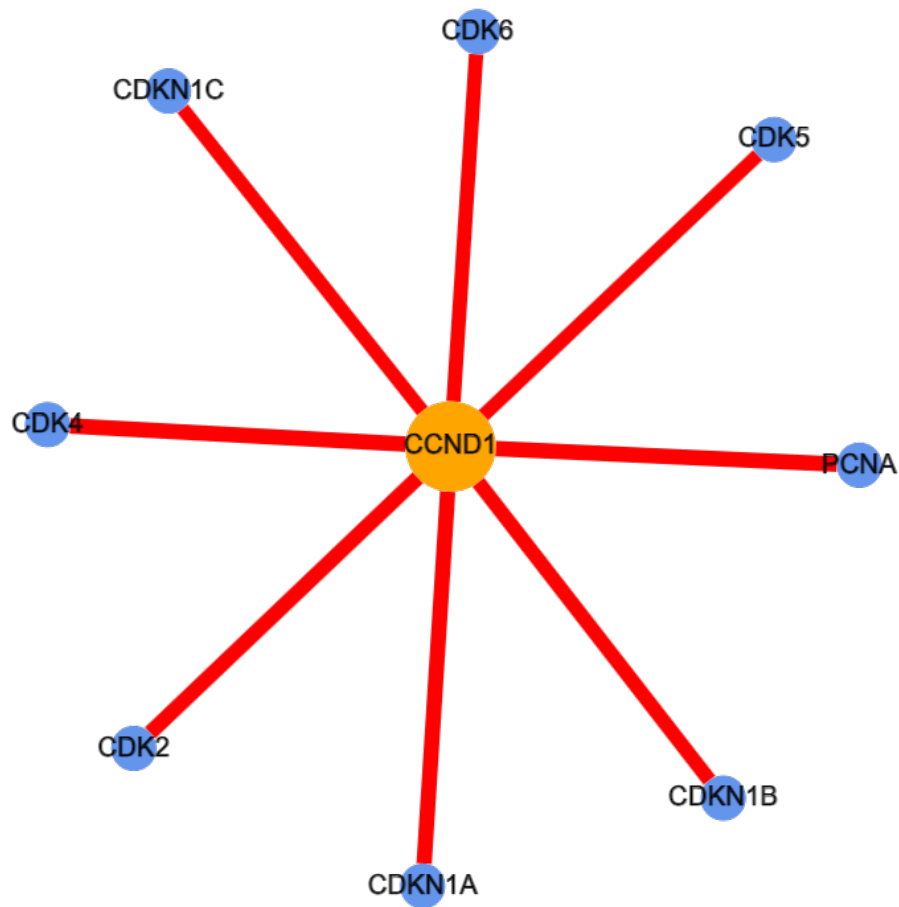
Supplementary figure S6. Volcano plot (left) and overrepresentation test result (right) of ccRCC proteomics dataset collected by DIA.



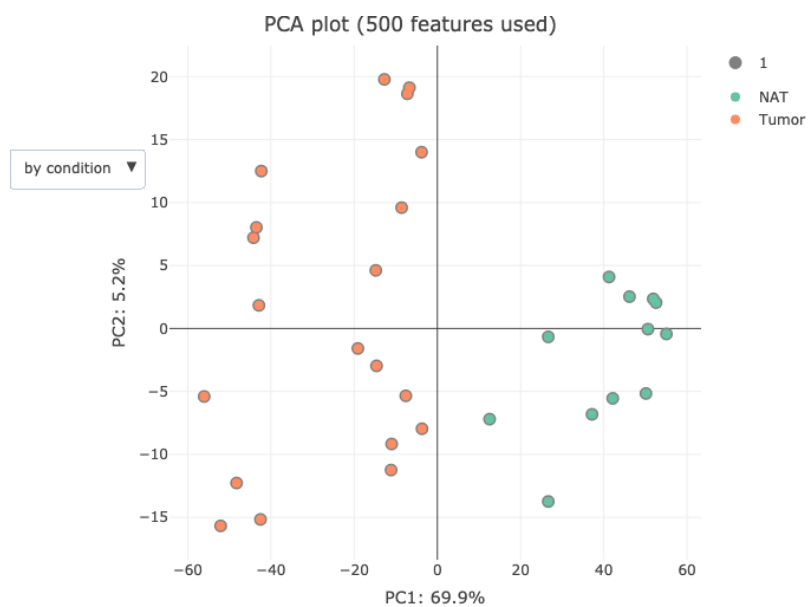
Supplementary figure S7. Scatter plot shows comparison of log₂ fold changes obtained from DIA and TMT experiments when comparing tumors versus NATs.



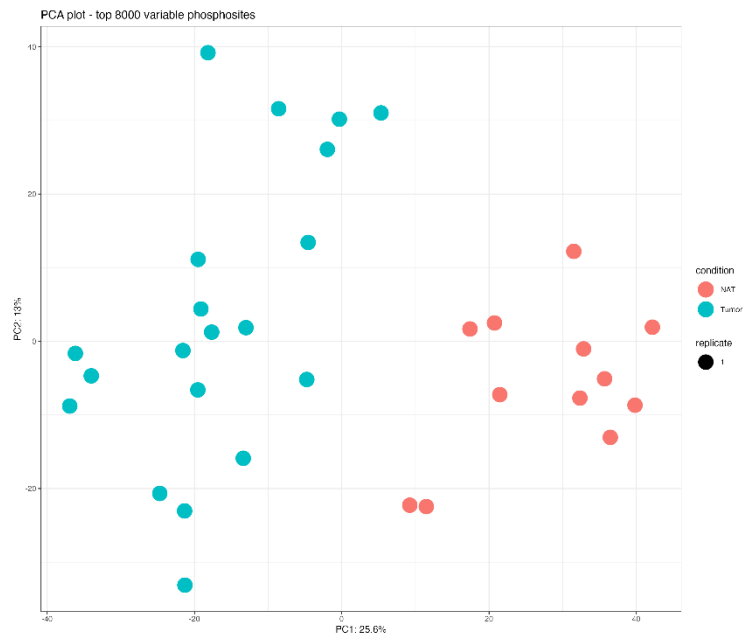
Supplementary figure S8. Density plot shows the imputation effect (Perseus style imputation) on AP-MS experiments.



Supplementary figure S9. Network visualization of HNSCC AP-MS dataset generated by SAINTexpress.



Supplementary figure S10. PCA plot of peptide-level analysis of ccRCC proteomics dataset.



Supplementary figure S13. PCA plot of ccRCC phosphoproteomics dataset after normalization.